A particle numerical approach based on the SPH method for Computational Fluid Mechanics

I. Colominas, L. Cueto-Felgueroso, G. Mosqueira, F. Navarrina, M. Casteleiro
Group of Numerical Methods in Engineering (http://caminos.udc.es/gmni)
Civil Engineering School, University of La Coruña, SPAIN

Abstract

Meshfree methods have experimented an important improvement in the last decade. Actually, we can say that the emerging meshless technology constitutes the most promising tool to simulate complex problems in the fluid dynamics area. In this paper we present a formulation which combines a Lagrangian description of the fluid movement (following the spirit of Smoothed Particle Hydrodynamics and Vortex Particle Methods) with a Galerkin formulation and Moving Least-Squares approximation. The performance of the methodology proposed is shown through various dynamic simulations, demonstrating the attractive ability of particle methods to handle severe distortions and complex phenomena.

1 Introduction

Meshless methods constitute a powerful and ambitious attempt to solve the equations of continuum mechanics without the computational workload associated to the explicit partition of the domain into certain non-overlapping cells. One of these techniques is the Smoothed Particle Hydrodynamics (SPH) method [1, 2], which was developed in the late 70's to simulate fluid dynamics in astrophysics [3, 4]. The extension to solid mechanics was introduced by Libersky, Petschek et al. [5] and Randles [6]. Johnson and Beissel proposed a Normalized Smoothing Function (NSF) algorithm [7] and other corrected SPH methods have been developed by Bonet et al. [8, 9] and Chen et al. [10]. More recently, Dilts has introduced Moving Least Squares (MLS) shape functions into SPH computations [11].

The ability of the Smoothed Particle Hydrodynamics method to handle severe distortions allows this technique to be succesfully applied to simulate fluid flows in CFD applications. Early SPH formulations included both a new approximation scheme and certain characteristic discrete equations (the so-called SPH equations), which may look quite strange for those researchers with some experience in methods with a higher degree of formalism such as finite elements. The formulation described in this paper follows a different approach, and the discrete equations are obtained using a Galerkin weighted residuals scheme. Although this new statement may result somewhat disconcerting for those accustomed to the classical SPH equations, the Galerkin formulation provides a strong framework to develop more consistent and stable algorithms.

2 MLS Shape Functions

One of the meshless interpolation scheme proposed for meshless approximations is the Moving Least Squares (MLS) method [12, 13]. Although different in their formulation, kernel based approximants (Moving Least Squares [14], Reproducing Kernel Particle Method [15]) can be seen as corrected SPH methods, and in practice they are very similar.

Let us consider a function $u(\boldsymbol{x})$ defined in a bounded, or unbounded, domain Ω. The basic idea of the MLS approach is to approximate $u(\boldsymbol{x})$, at a given point $\boldsymbol{x}$, through a polynomial least-squares fitting of $u(\boldsymbol{x})$ in a neighbourhood of $\boldsymbol{x}$ as:

$$u(\boldsymbol{x}) \approx \widehat{u}(\boldsymbol{x}) = \sum_{i=1}^{m} p_i(\boldsymbol{x})\alpha_i(\boldsymbol{z})\Big|_{\boldsymbol{z}=\boldsymbol{x}} = \boldsymbol{p}^t(\boldsymbol{x})\boldsymbol{\alpha}(\boldsymbol{z})\Big|_{\boldsymbol{z}=\boldsymbol{x}} \tag{1}$$

where $\boldsymbol{p}^t(\boldsymbol{x})$ is an m-dimensional polynomial basis and $\boldsymbol{\alpha}(\boldsymbol{z})\Big|_{\boldsymbol{z}=\boldsymbol{x}}$ is a set of parameters to be determined, such that they minimize the following error functional:

$$J(\boldsymbol{\alpha}(\boldsymbol{z})\Big|_{\boldsymbol{z}=\boldsymbol{x}}) = \int_{\boldsymbol{y}\in\Omega_{\boldsymbol{x}}} W(\boldsymbol{z}-\boldsymbol{y},h)\Big|_{\boldsymbol{z}=\boldsymbol{x}} \left[u(\boldsymbol{y}) - \boldsymbol{p}^t(\boldsymbol{y})\boldsymbol{\alpha}(\boldsymbol{z})\Big|_{\boldsymbol{z}=\boldsymbol{x}}\right]^2 d\Omega_{\boldsymbol{x}} \tag{2}$$

where $W(\boldsymbol{z}-\boldsymbol{y},h)\Big|_{\boldsymbol{z}=\boldsymbol{x}}$ is a symmetric kernel with compact support (denoted by $\Omega_{\boldsymbol{x}}$) chosen among the kernels used in standard SPH, and the smoothing length h measures the size of $\Omega_{\boldsymbol{x}}$. The stationary conditions of J with respect to $\boldsymbol{\alpha}$ lead to

$$\int_{\boldsymbol{y}\in\Omega_{\boldsymbol{x}}} \boldsymbol{p}(\boldsymbol{y})W(\boldsymbol{z}-\boldsymbol{y},h)\Big|_{\boldsymbol{z}=\boldsymbol{x}}\, u(\boldsymbol{y})d\Omega_{\boldsymbol{x}} = \boldsymbol{M}(\boldsymbol{x})\boldsymbol{\alpha}(\boldsymbol{z})\Big|_{\boldsymbol{z}=\boldsymbol{x}} \tag{3}$$

where the moment matrix $\boldsymbol{M}(\boldsymbol{x})$ is

$$\boldsymbol{M}(\boldsymbol{x}) = \int_{\boldsymbol{y}\in\Omega_{\boldsymbol{x}}} \boldsymbol{p}(\boldsymbol{y})W(\boldsymbol{z}-\boldsymbol{y},h)\Big|_{\boldsymbol{z}=\boldsymbol{x}}\, \boldsymbol{p}^t(\boldsymbol{y})d\Omega_{\boldsymbol{x}} \tag{4}$$

In numerical computations, the global domain Ω is discretized by a set of n nodes or particles, and the integrals in (3) and (4) can be computed by using those

nodes inside $\Omega_{\boldsymbol{x}}$ as quadrature points (nodal integration). Thus, rearranging (3) we can write

$$\boldsymbol{\alpha}(\boldsymbol{z})\Big|_{\boldsymbol{z}=\boldsymbol{x}} = \boldsymbol{M}^{-1}(\boldsymbol{x})\boldsymbol{P}_{\Omega_{\boldsymbol{x}}}\boldsymbol{W}_V(\boldsymbol{x})\boldsymbol{u}_{\Omega_{\boldsymbol{x}}} \tag{5}$$

where the vector $\boldsymbol{u}_{\Omega_{\boldsymbol{x}}}$ contains certain nodal parameters of those nodes in $\Omega_{\boldsymbol{x}}$, and $\boldsymbol{M}(\boldsymbol{x}) = \boldsymbol{P}_{\Omega_{\boldsymbol{x}}}\boldsymbol{W}_V(\boldsymbol{x})\boldsymbol{P}^t_{\Omega_{\boldsymbol{x}}}$, being

$$\boldsymbol{P}_{\Omega_{\boldsymbol{x}}} = \left(\boldsymbol{p}(\boldsymbol{x}_1)\,\boldsymbol{p}(\boldsymbol{x}_2)\,\cdots\,\boldsymbol{p}(\boldsymbol{x}_{n_{\boldsymbol{x}}})\right);\ \boldsymbol{W}_V(\boldsymbol{x}) = diag\left\{W_i(\boldsymbol{x}-\boldsymbol{x}_i)V_i\right\},\ i=1,n_{\boldsymbol{x}} \tag{6}$$

The complete details can be found in [15]. In the above equations, $n_{\boldsymbol{x}}$ denotes the total number of nodes within the neighbourhood of point $\boldsymbol{x}$ and V_i and $\boldsymbol{x}_i$ are, respectively, the tributary volume (used as quadrature weight) and the coordinates associated to node i. Note that the tributary volumes of neighbouring nodes are included in the matrix $\boldsymbol{W}_V$, obtaining the MLS Reproducing Kernel Particle Method [15]. Otherwise, we can use $\boldsymbol{W}$ instead of $\boldsymbol{W}_V$ being

$$\boldsymbol{W}(\boldsymbol{x}) = diag\left\{W_i(\boldsymbol{x}-\boldsymbol{x}_i)\right\}, \qquad i=1,\ldots,n_{\boldsymbol{x}} \tag{7}$$

which corresponds to the classical MLS approximation (in the nodal integration of the functional (2), the same quadrature weight is associated to all nodes). Introducing (5) in (1) the interpolation structure can be identified as:

$$\widehat{u}(\boldsymbol{x}) = \boldsymbol{p}^t(\boldsymbol{x})\mathrm{M}^{-1}(\boldsymbol{x})\boldsymbol{P}_{\Omega_{\boldsymbol{x}}}\boldsymbol{W}_V(\boldsymbol{x})\boldsymbol{u}_{\Omega_{\boldsymbol{x}}} = \boldsymbol{N}^t(\boldsymbol{x})\boldsymbol{u}_{\Omega_{\boldsymbol{x}}} \tag{8}$$

And, therefore, the MLS shape functions can be written as:

$$\boldsymbol{N}^t(\boldsymbol{x}) = \boldsymbol{p}^t(\boldsymbol{x})\mathrm{M}^{-1}(\boldsymbol{x})\boldsymbol{P}_{\Omega_{\boldsymbol{x}}}\boldsymbol{W}_V(\boldsymbol{x}) \tag{9}$$

It is most frequent to use a scaled and locally defined polinomial basis, instead of the globally defined $\boldsymbol{p}(\boldsymbol{y})$. Thus, if a function is to be evaluated at point $\boldsymbol{x}$, the basis would be of the form $\boldsymbol{p}(\frac{\boldsymbol{y}-\boldsymbol{x}}{h})$. The shape functions are, therefore, of the form

$$\boldsymbol{N}^t(\boldsymbol{x}) = \boldsymbol{p}^t(\boldsymbol{0})\mathrm{M}^{-1}(\boldsymbol{x})\boldsymbol{P}_{\Omega_{\boldsymbol{x}}}\boldsymbol{W}_V(\boldsymbol{x}) \tag{10}$$

In the examples presented in this paper, a linear polynomial basis has been used, which provides linear completeness. Respect to the choice of kernel, a wide variety of kernel functions have been proposed in the literature, most of them being spline or exponential functions. We have not found a general criterion for an optimal choice and we use a cubic spline [12, 13].

3 Discrete Equations for Fluid Flow Problems

3.1 Weighted residuals. Test and trial functions.

We assume that the behaviour of a continuum can be analyzed by means of the following governing equations: the continuity equation (conservation of mass) and the momentum equation (conservation of linear momentum) [12, 13].

The meshless discrete equations can be derived using a weighted residuals formulation. Thus, the global weak (integral) form of the spatial momentum equation can be written as:

$$\int_\Omega \rho \frac{d\widehat{\boldsymbol{v}}}{dt} \cdot \delta\widehat{\boldsymbol{v}}\, d\Omega = -\int_\Omega \widehat{\boldsymbol{\sigma}} : \delta\widehat{\boldsymbol{l}}\, d\Omega + \int_\Omega \boldsymbol{b} \cdot \delta\widehat{\boldsymbol{v}}\, d\Omega + \int_\Gamma \widehat{\boldsymbol{\sigma}}\boldsymbol{n} \cdot \delta\widehat{\boldsymbol{v}}\, d\Gamma \tag{11}$$

where Ω is the problem domain, Γ is its boundary, and certain functions $\delta\widehat{\boldsymbol{v}}$ and $\widehat{\boldsymbol{v}}$ are the approximations to the test and trial functions $\delta\boldsymbol{v}$ and $\boldsymbol{v}$.

The spatially discretized equations are obtained after introducing meshless test and trial functions and their gradients in (11) as

$$\delta\widehat{\boldsymbol{v}}(\boldsymbol{x}) = \sum_{i=1}^{n} \delta\boldsymbol{v}_i N_i^*(\boldsymbol{x}), \qquad \boldsymbol{\nabla}\delta\widehat{\boldsymbol{v}}(\boldsymbol{x}) = \sum_{i=1}^{n} \delta\boldsymbol{v}_i \otimes \nabla_{\boldsymbol{x}} N_i^*(\boldsymbol{x}) \tag{12}$$

$$\widehat{\boldsymbol{v}}(\boldsymbol{x}) = \sum_{j=1}^{n} \boldsymbol{v}_j N_j(\boldsymbol{x}), \qquad \boldsymbol{\nabla}\widehat{\boldsymbol{v}}(\boldsymbol{x}) = \sum_{j=1}^{n} \boldsymbol{v}_j \otimes \nabla_{\boldsymbol{x}} N_j(\boldsymbol{x}). \tag{13}$$

Thus, for each node (particle) i the following identity must hold:

$$\sum_{j=1}^{n} \int_\Omega m_{ij} \frac{d\boldsymbol{v}_j}{dt} = \boldsymbol{f}_i^{int} + \boldsymbol{f}_i^{ext}, \qquad i = 1, n \tag{14}$$

where the mass term m_{ij}, the internal forces term $\boldsymbol{f}_i^{int}$ and the external forces term $\boldsymbol{f}_i^{ext}$ are:

$$m_{ij} = \int_\Omega \rho N_i^*(\boldsymbol{x}) N_j(\boldsymbol{x}) d\Omega \tag{15}$$

$$\boldsymbol{f}_i^{int} = -\int_\Omega \widehat{\boldsymbol{\sigma}} \boldsymbol{\nabla}_{\boldsymbol{x}} N_i^*(\boldsymbol{x}) d\Omega, \quad \boldsymbol{f}_i^{ext} = \int_\Omega N_i^*(\boldsymbol{x}) \boldsymbol{b}\, d\Omega + \int_\Gamma N_i^*(\boldsymbol{x}) \widehat{\boldsymbol{\sigma}}\boldsymbol{n}\, d\Gamma \tag{16}$$

The MLS shape functions do not vanish on essential boundaries and, therefore, the boundary integral in (16) can be decomposed as:

$$\int_\Gamma N_i^*(\boldsymbol{x}) \widehat{\boldsymbol{\sigma}}\boldsymbol{n}\, d\Gamma = \int_{\Gamma_u} N_i^*(\boldsymbol{x}) \widehat{\boldsymbol{\sigma}}\boldsymbol{n}\, d\Gamma_u + \int_{\Gamma_n} N_i^*(\boldsymbol{x}) \widehat{\boldsymbol{\sigma}}\boldsymbol{n}\, d\Gamma_n \tag{17}$$

being Γ_u and Γ_n, respectively, the parts of the boundary where essential and natural boundary conditions are prescribed and $\Gamma = \Gamma_u \cup \Gamma_n$. It is important to remark that imposing the boundary conditions is one of the most important and problematic issues in SPH methods, since they can not be enforced as directly as in finite elements. Natural boundary conditions are included in the weak form through the boundary traction term, and at this point the "only" difficulty is the determination of the boundary particles and their weights. Unfortunately, the test functions do not vanish on essential boundaries, and a term including tractions on essential boundaries remains in the weak form of the problem. A more extensive study about this topic can be found in [12].

Regarding the equation used for mass conservation, its Galerkin weak form is equivalent to a point collocation scheme and, thus, the continuity equation must be enforced at each particle i,

$$\frac{d\rho_i}{dt} = -\rho_i div(\boldsymbol{v})_i = -\rho_i \sum_{j=1}^{n} \boldsymbol{v}_j \cdot \boldsymbol{\nabla}_{\boldsymbol{x}} N_j(\boldsymbol{x}_i) \tag{18}$$

where expression (13) for $\boldsymbol{\nabla}\widehat{\boldsymbol{v}}_i$ has been used.

3.2 Numerical Integration

An important issue in meshless methods corresponds to the numerical integration of the weak form, being also the source of well-known inaccuracies and instabilities [9, 12, 14]. The main aspects that must be considered when choosing a numerical quadrature for particle methods are: *i)* the method should provide reasonable accuracy, *ii)* the numerical quadrature should retain the meshless character of the method, and *iii)* it should be computationally efficient.

Numerical integration –which concerns the nature itself of meshless methods— has received much attention in Galerkin-based meshless formulations (e.g., the EFGM [2]) but it has not been explicitly studied in SPH, probably because nodal integration lies in the basis of its early formulations and the method was considered a collocation method. Nodal integration has been used, at least implicitly, in all SPH formulations [1, 8], and it evidently is the cheapest option that leads to a truly meshless resulting scheme. The nodes are used as quadrature points and the corresponding integration weights are their tributary volumes. However, this integration scheme is also the cause of instabilities in the numerical solution [9, 14].

To overcome these problems, some alternatives have been proposed. In the EFG and RKPM methods, it is frequently defined a background integration mesh composed by non overlapping cells that cover the whole domain (Figure 1.a), where high order Gauss quadratures are defined [2]. Although these cells do not generally match the integration domains, the spatial framework required by the Galerkin method is recovered (obviously at the cost of the generation of an integration mesh).

In the context of SPH, alternative numerical quadratures have been proposed within the concept of “stress-points”. The idea is essentially to “calculate stresses away from the centroids (the nodes)”, that is, to use a quadrature other than nodal integration in the Galerkin weak form. Then, we must deal with two sets of points: the particles (or nodes) where the MLS-interpolation is defined, and the integration points (the “stress points”), spread among the cloud of particles with no reference to any background mesh (Figure 1.b). Stress points are set up in certain positions and their movement is completely determined by the movement of the particles.

More recently, Belytschko and coworkers [14] have reinterpreted SPH as a nodally integrated Galerkin method. Following a similar approach, in the context of Galerkin methods, the question about SPH and numerical integration gains full sense, providing a clear framework to analyze the use of the “stress-points”.

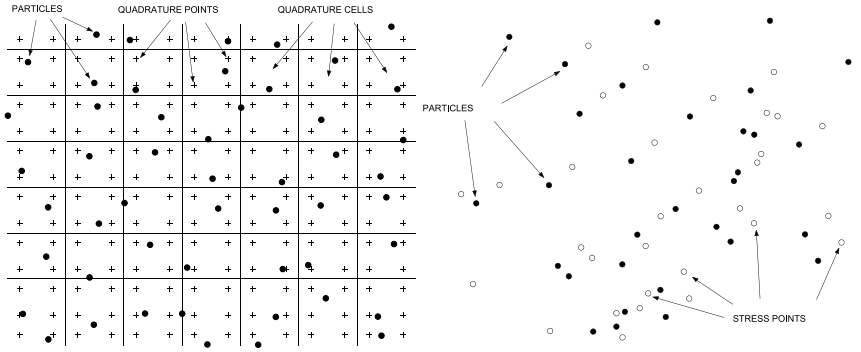

Figure 1: Numerical integration: **a)** Background mesh; **b)** Particles and stress-points (doble grid)

In references [12, 13] it can be found an extensive revision of these concepts, such as the difference between particle and mesh-based methods regarding numerical integration, the nodal integration in the context of the SPH methods, the use of a background integration mesh, the concept of "stress-points" and a new proposal for a more efficient implementation of "stress-points".

Taking into account these aspects about the numerical integration, we can now write the complete spatially discretized set of equations for a generic integration method. In the following development, we assume a Bubnov-Galerkin scheme where both, the test and trial functions, are chosen from the same space.

For the momentum equation, in practical applications it is not efficient to use the complete mass matrix. Thus, lumped mass matrices are most frequently used. A simple lumping technique corresponds to a row-sum mass matrix; then the discrete counterpart of the lumped mass term M_i associated to particle i is

$$M_i = \sum_{k=1}^{ninte} \rho_k N_i^*(\boldsymbol{x}_k) W_k \tag{19}$$

provided that trial functions are, at least, zeroth order complete. If test functions are also zeroth order complete, this lumping is moreover consistent [12]. Taking into account this lumping, the momentum equation results as

$$M_i \frac{d\boldsymbol{v}_i}{dt} = \widehat{\boldsymbol{f}}_i^{int} + \widehat{\boldsymbol{f}}_i^{ext}, \qquad i = 1, n \tag{20}$$

where $\widehat{\boldsymbol{f}}_i^{int}$ and $\widehat{\boldsymbol{f}}_i^{ext}$ are the discrete version of the forces terms (16):

$$\widehat{\boldsymbol{f}}_i^{int} = -\sum_{k=1}^{ninte} \widehat{\boldsymbol{\sigma}}_k \boldsymbol{\nabla} N_i(\boldsymbol{x}_k) W_k, \;\; \widehat{\boldsymbol{f}}_i^{ext} = \sum_{k=1}^{ninte} N_i(\boldsymbol{x}_k) \boldsymbol{b}_k W_k + \sum_{k=1}^{ninte^B} N_i(\boldsymbol{x}_k) \widehat{\boldsymbol{\sigma}}_k \boldsymbol{n} W_k^B \tag{21}$$

where $ninte$ is the total number of quadrature points and $ninte^B$ is the number of boundary integration points. Note that appropriate weights, W_k and W_k^B, must be defined for interior and boundary quadrature points [12].

Now, assuming a compressible newtonian fluid and eulerian kernels [12, 13], the internal forces are related to the Cauchy stress tensor which must be computed at each quadrature point,

$$\widehat{\boldsymbol{\sigma}}_k = -p_k \boldsymbol{I} + 2\mu_k \widehat{\boldsymbol{d}}_k' \tag{22}$$

where p_k is the pressure, μ_k is the viscosity and $\widehat{\boldsymbol{d}}_k'$ is related to the velocity gradient tensor [12].

Finally, the continuity equation results as

$$\frac{d\rho_i}{dt} = -\rho_i \, div(\boldsymbol{v})_i = -\rho_i \sum_{j=1}^{n} \boldsymbol{v}_j \cdot \boldsymbol{\nabla} N_j(\boldsymbol{x}_i) \tag{23}$$

In references [12, 13], it can be found some additional aspects of this numerical approach, such as the performance of the particles movement, the enforcement of the essential boundary conditions, the initialization of the field variables, different alternatives for the discrete equations, the time integration algorithm proposed, and a schematic flowchart and several remarks about the practical implementation of the exposed methodology.

4 Examples and Conclusions

The first example is a simulation corresponding to the filling of a circular mould with core (Figure 2). The velocity of the jet at the gate is $18\ m/s$ and the viscosity is $\mu = 0.01\ kg\ m^{-1}s^{-1}$. The bulk modulus κ was chosen such that the wave celerity is $1000\ m/s$ and the total number of particles is 14314. In Figure 3, two instants of the numerical simulation are shown and compared to the obtained by Schmid and Klein [16].

The next example is a fluid-structure interaction problem: the opening of a lock-gate which retains a fluid. The simulation corresponds to the flow of the fluid as the gate rises at a constant speed of $0.7\ m\ s^{-1}$. Figure 4 shows the initial configuration and the simulations at different stages.

The results obtained demonstrate the ability of the proposed numerical approach to simulate complex unsteady fluid flow problems. The Galerkin approach constitutes a clear framework to derive the discrete equations, while a moving least squares approximation significantly improves the standard smooth particle hydrodynamics kernel estimates. Within this general methodology it is possible to explain from a rigorous point of view some of the corrections that are generally introduced in the SPH method to obtain accurate solutions. Furthermore, it is now possible to derive new more consistent and stable meshless numerical approaches.

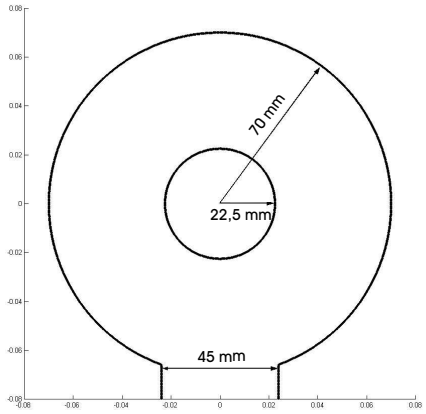

Figure 2: Mould filling: Dimensions of the mould.

Acknowledgments

This work has been partially supported by the SGPICT of the "Ministerio de Ciencia y Tecnología" of the Spanish Government (Grant DPI# 2001-0556), the "Xunta de Galicia" (Grant # PGDIT01PXI11802PR) and the University of La Coruña.

References

[1] J.J. Monaghan. Introduction to SPH. *Comp.Phys.Comm.* **48**:89–96 (1988).

[2] T. Belytschko, Y.Y. Lu, L. Gu. Element-Free Galerkin methods. *Int.J.Num.Met.Engrg.* **37**:229–256 (1994).

[3] L.B. Lucy. A numerical approach to the testing of the fission hypothesis. *Astron.J.* **82**:1013 (1977).

[4] R.A. Gingold, J.J. Monaghan. SPH: theory and application to non-spherical stars. *Month.Not.Roy.Astron.Soc.* **181**:378 (1977).

[5] L.D. Libersky, A.G. Petschek, T.C. Carney, J.R. Hipp, F.A. Allahdadi. High strain Lagrangian hydrodynamics. *J.Comp.Phys.* **109**:67–75 (1993).

[6] P.W. Randles, L.D. Libersky. SPH: Some recent improvements and applications. *Comp.Met.Appl.Mech.Engrg.* **139**:375–408 (1996).

[7] G.R. Johnson, S.R. Beissel. Normalized Smoothing Functions for SPH impact computations. *Int.J.Num.Met.Engrg.* **39**:2725–2741 (1996).

[8] J. Bonet, T-S.L. Lok. Variational and momentum preserving aspects of SPH formulations. *Comp.Met.Appl.Mech.Engrg.* **180**:97–115 (1999).

[9] J. Bonet, S. Kulasegaram. Correction and stabilization of SPH with applications in metal forming. *Int.J.Num.Met.Engrg.* **47**:1189–1214 (2000).

[10] J.K. Chen, J.E. Beraun. A generalized SPH method for nonlinear dynamic problems. *Comp.Met.Appl.Mech.Engrg.* **190**:225–239 (2000).

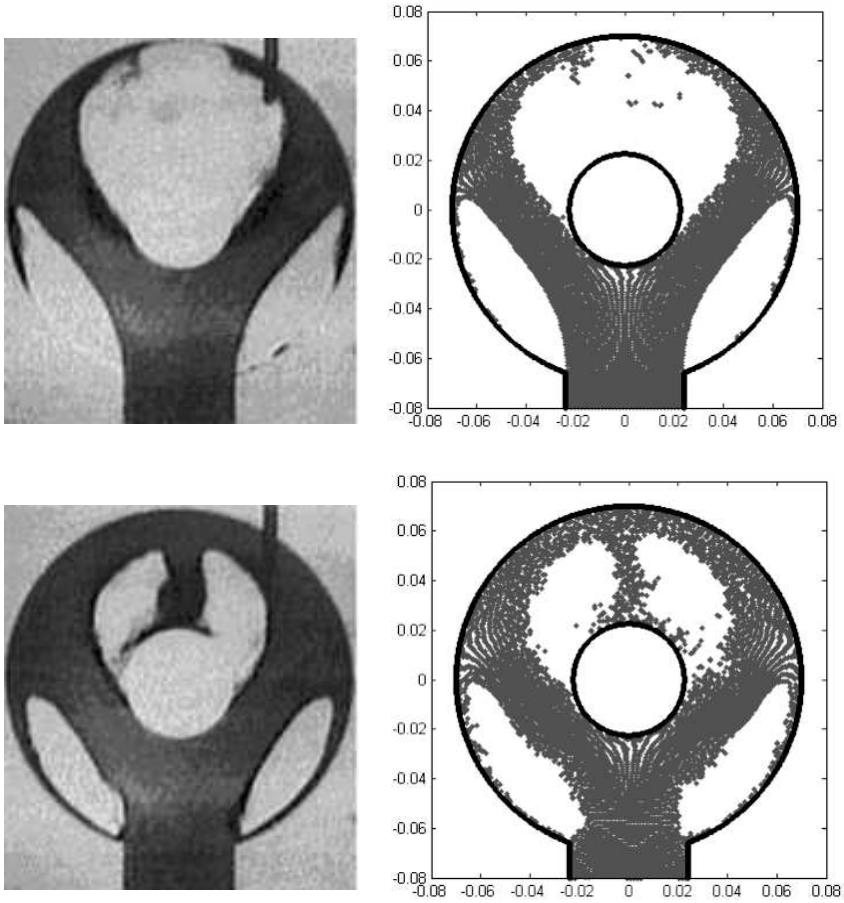

Figure 3: Mould filling:Experimental (left) and numerical (right) results.

[11] G.A. Dilts. MLS Particle Hydrodynamics. *Int.J.Num.Met.Engrg.* Part I **44**: 1115-1155 (1999), Part II **48**: 1503 (2000).

[12] L.Cueto-Felgueroso, I.Colominas,G.Mosqueira, F.Navarrina, M.Casteleiro. On the Galerkin formulation of SPH. *Int.J.Num.Met.Engrg.* [press] (2004).

[13] L. Cueto-Felgueroso. A unified analysis of meshless methods: formulation & applications. Technical Report (in Spanish), Univ. de La Coruña, (2002).

[14] T. Belytschko, Y. Guo, W.K. Liu, S.P. Xiao. A unified stability analysis of meshless particle methods. *Int.J.Num.Met.Engrg.* **48**:1359–1400 (2000).

[15] W.K. Liu, S. Li, T. Belytschko. MLS Reproducing Kernel methods (I). *Comp.Met.Appl.Mech.Engrg.* **143**:113–154 (1997).

[16] M. Schmid, F. Klein. Fluid flow in die cavities - experimental and numerical simulation, NADCA 18. *Int. Die Casting Congress.* Indianapolis (1995).

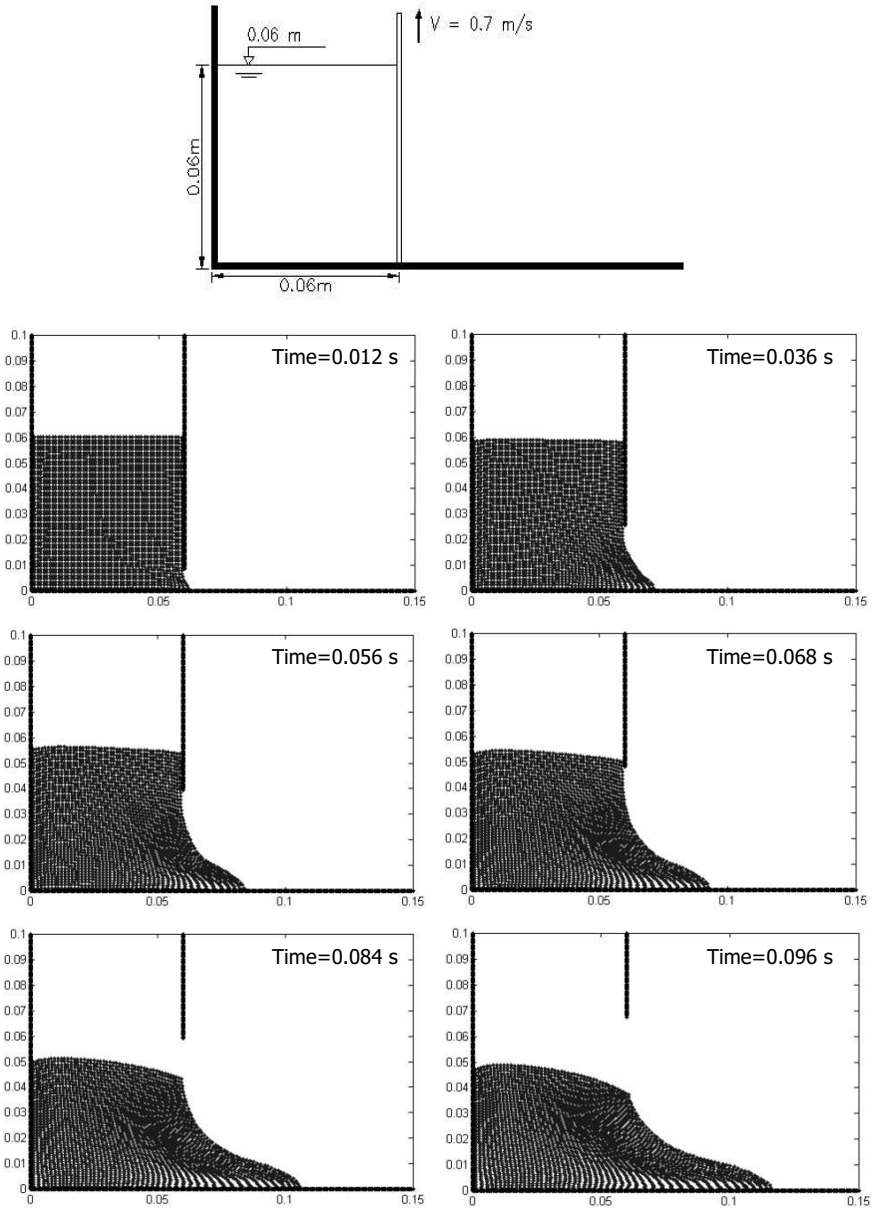

Figure 4: Lockgate opening: Initial configuration and simulation at various stages.